Sensory-evoked synaptic integration in cerebellar and cerebral cortical neurons

Paul Chadderton[1], Andreas T. Schaefer[2,3], Stephen R. Williams[4] and Troy W. Margrie[2,3]

Abstract | Neurons integrate synaptic inputs across time and space, a process that determines the transformation of input signals into action potential output. This article explores how synaptic integration contributes to the richness of sensory signalling in the cerebellar and cerebral cortices. Whether a neuron receives a few or a few thousand discrete inputs, most evoked synaptic activity generates only subthreshold membrane potential fluctuations. Sensory tuning of synaptic inputs is typically broad, but short-term dynamics and the interplay between excitation and inhibition restrict action potential firing to narrow windows of opportunity. We highlight the challenges and limitations of the use of somatic recordings in the study of synaptic integration and the importance of active dendritic mechanisms in sensory processing.

[1]*Department of Bioengineering, Imperial College London, London, SW7 2AZ, UK.*
[2]*Department of Neuroscience, Physiology and Pharmacology, University College London, Gower Street, London, WC1E 6BT, UK.*
[3]*The Division of Neurophysiology, MRC National Institute for Medical Research, Mill Hill, London, NW7 1AA, UK.*
[4]*The Queensland Brain Institute, The University of Queensland, St Lucia, Queensland, 4072, Australia.*
Correspondence to P.C., A.T.S. and T.W.M.
e-mails: p.chadderton@imperial.ac.uk; aschaef@nimr.mrc.ac.uk; troy.margrie@nimr.mrc.ac.uk
doi:10.1038/nrn3648
Published online
17 January 2014

Neurons are informed about the world via their synapses. The information conveyed via synaptic inputs determines if and when a neuron will fire an action potential and thus contribute to interneuronal communication. To study the integration of these signals, it is necessary to record the fluctuations in the membrane potential of the cell intracellularly, as synaptic transmission causes electrical fluctuations that are virtually invisible outside the neuron. The application of *in vivo* whole-cell patch clamp recording and two-photon imaging has led to a rapid growth in the study of sensory-evoked synaptic activity at the level of single neurons[1–17], particularly in rodents; but how close are we to understanding the intricate relationship between sensory-evoked synaptic input and action potential output in the intact brain?

Depending on its cell type, a given neuron may be required to process signals from anywhere between a few up to many thousands of synapses. The integration of these signals lies at the heart of sensory processing and neural computation. In this Review, we examine our current understanding of the mechanisms that are used to convey essential sensory information within single cells. We focus on synaptic integration in the most numerous neuronal types of the cerebellar cortex (cerebellar granule cells) and the cerebral cortex (cortical pyramidal cells).

Multisensory cerebellar granule cells

Granule cells are the smallest neurons in the brain and constitute the input layer of the cerebellar cortex. They receive only a handful of excitatory connections (from three to seven) onto a few short dendrites[18] (FIG. 1A); this makes it possible to isolate individual synaptic responses via recordings at the cell body[19] and so to directly investigate their individual contribution to sensory computation at the level of a single cell.

Phasic versus tonic responses. In granule cells, the patterning of spontaneous and sensory-evoked synaptic activity varies across cerebellar regions and reflects how mossy fibre–granule cell synapses encode unique information to a given sensory modality[20–26]. In somatosensory areas, whisker and perioral[20,22,26] or forepaw stimulation[21,24] evokes brief bursts of synaptic inputs that instantaneously reach frequencies of many hundreds of hertz. Responses to these stimuli tend to show similar characteristics: the amplitude of synaptic currents progressively decreases during sensory-evoked bursts, and the response does not persist beyond the duration of the stimulus. In the absence of overt stimulation, these synapses are largely quiescent[20], which ensures a high signal-to-noise ratio when salient stimuli are generated.

By contrast, granule cells that receive proprioceptive signals resulting from joint rotation[21], whole-body

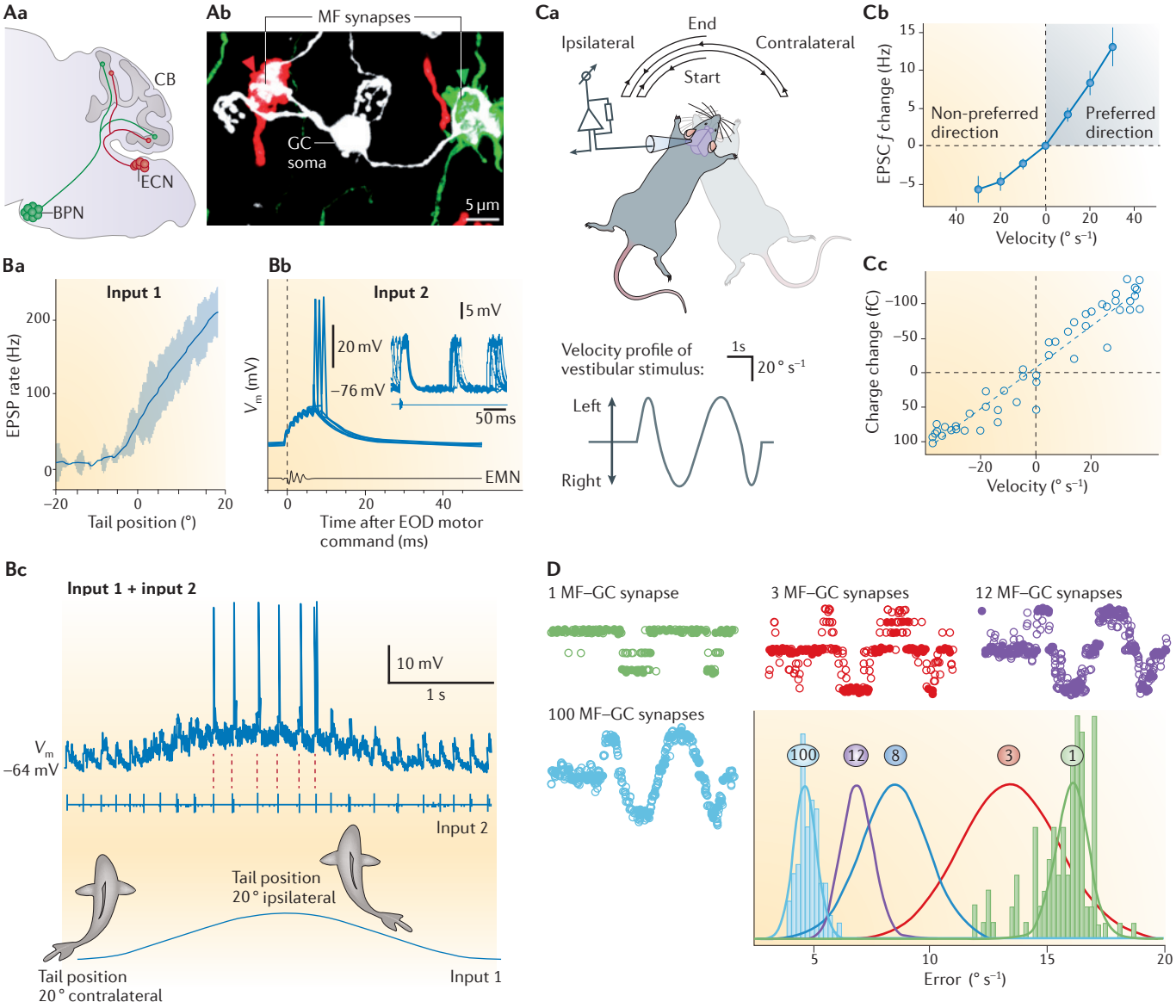

Figure 1 | **Sensory integration and stimulus reconstruction in simple cells.** **Aa** | A schematic showing the injection sites for adeno-associated virus (AAV) labelling of two distinct mossy fibre (MF) pathways onto individual granule cells (GCs) in the mouse. **Ab** | Inputs from both the external cuneate nucleus (ECN, red) and basilar pontine nucleus (BPN, green) can converge onto the same GC. **Ba** | Recordings from GCs in fish show monotonic modulations in the excitatory postsynaptic potential (EPSP) rate during tail movement. **Bb** | In the same cell, phasic discharge of EPSPs following electric organ discharge (EOD) can be observed. Typically, such responses remain at subthreshold levels. The bottom trace is an electric motor neuron (EMN) volley recorded near the electric organ. **Bc** | Only coincident activation of both inputs results in the discharge of an action potential. **Ca–c** | Similarly, recordings from the mouse cerebellar flocculus show linear changes in EPSP frequency in response to angular rotation (and vestibular activation (**Cb**)). Synaptic responses show no short-term dynamics in amplitude or net charge (**Cc**). **D** | A reconstruction of the vestibular stimulus (black trace in the bottom panel of **Ca**) using Bayesian analysis and data recorded from floccular GCs showing stimulus reconstruction for 1, 3, 12 and 100 MF–GC synapses. CB, cerebellum. Part **A** is reproduced from REF. 27. Part **B** is reproduced, with permission, from REF. 25 © (2010) Elsevier. Parts **C** and **D** are reproduced, with permission, from REF. 23 © (2008) American Association for the Advancement of Science.

Postsynaptic potential (PSP). A fluctuation in the membrane potential owing to the binding of excitatory transmitter molecules (glutamate) and/or inhibitory transmitter molecules (glycine and GABA) that are released from axon terminals following a presynaptic action potential.

rotation[23] or, in fish, tail position[25] exhibit comparatively high rates of spontaneous synaptic activity and display more tonic responses to changes in the sensory world. In fish, movement of the tail or chin appendage results in modulation of the frequency of synaptic responses so that the postsynaptic potential (PSP) rate is highest at one extreme position and lowest at the other (FIG. 1B). Similarly, in the mouse cerebellar flocculus, where vestibular information is processed, the direction and velocity of horizontal rotation is represented as a change in the rate of activity at individual mossy fibre synapses (FIG. 1C). A moderate rate of spontaneous activity at these synapses enables the representation of the velocity of motion to be signalled as a linear increase or decrease in frequency to

indicate the direction of movement. In addition, during rotation in the preferred direction, the velocity of motion may be approximated by the rate of excitatory postsynaptic currents that show no short-term dynamics over a wide range of velocities. In this way, the synaptic signal is maintained with remarkable reliability across a range of stimulus intensities.

Coincidence detection of multimodal events. Despite receiving only a small number of inputs, individual granule cells carry out computations such as multimodal stimulus coincidence detection. Anatomical studies indicate that granule cells can receive inputs from distinct sensorimotor pathways[27] (FIG. 1A) and support electrophysiological evidence from the flocculus[23], demonstrating that only one of a handful of available synapses is dedicated to reporting the activation of the horizontal semicircular canals.

In fish, the mechanisms of integration of distinct sensorimotor-encoding synapses reporting discharge from the electric organ and body position have been characterized[25]. Passive displacement of the tail results in modulation of the tonically active input, whereas discharge from the electric organ produces a large phasic PSP. Typically, neither the summating tail position-encoding PSPs nor the electric organ discharge causes the granule cell to fire. Rather, the combined activation of the two inputs is necessary to drive output, such that action potential activity only encodes body position during a narrow time window immediately after electric organ discharge[25].

Stimulus reconstruction by individual synapses. One advantage of being able to isolate and track the activity of individual synaptic inputs is that it becomes possible to explore the contribution of an individual synapse to stimulus reconstruction at the cell and circuit level. In the case of vestibular-encoding synapses, the amplitude and charge of synaptic responses, when averaged over a broad range of inter-event intervals, (FIG. 1C) have been found to be invariant and reflect a reliable velocity encoder[23].

Although this average-based analysis gives an indication of what these synaptic events represent, it does not provide insight into the usefulness of the instantaneous signal, as is the requirement under real-world conditions. A Bayesian approach to stimulus reconstruction, which is based on the recorded frequencies of vestibular-evoked synaptic responses, has shown the exquisite sensitivity of these transmitted signals. In a given granule cell, the frequency of activity at an individual synapse over a single-stimulus trial reliably reports the direction of whole-body rotation, whereas estimates of the velocity report substantial error. By simply adding increasing numbers of trials of synaptic responses recorded either in the same granule cell or in different granule cells, an accurate readout of velocity is obtained with a mere 100 mossy fibre–granule cell synapses distributed across the input layer of the cerebellar network[23] (FIG. 1D).

Such experimental and theoretical data obtained for the humble granule cell indicate that synaptic processing in the input layer to the cerebellum underlies the mechanistic operations that are designed to generate sparse and selective postsynaptic output patterns[28–31]. Stimulus onset and intensity are accurately reported at the level of individual synapses, and the reliability of these synapses means that only a few hundred granule cells may be required for a complete neuronal reconstruction of a sensory stimulus. Synaptic inputs can therefore generate linear representations of stimulus features[23], but in many situations this is not the case[20–22,25]. Furthermore, the linearity of the input–output function during active sensory processing is yet to be established. Recordings from granule cells will continue to provide precious insight into how the integration of individual synaptic inputs imposes functionality and specificity in a vast sea of input-layer neurons.

Sensory integration in pyramidal cells

At the other end of the complexity spectrum, neocortical pyramidal neurons receive thousands of inputs[32] across an extensive dendritic tree. Representations of the sensory world are conveyed to individual pyramidal cells via the overlapping activation of numerous synaptic inputs that result in synaptic receptive fields being broadly tuned (BOX 1). Unitary synaptic inputs onto pyramidal cells are very small when measured at the soma (rarely exceeding a few hundred microvolts) and usually can only be isolated in somatic recordings *in vivo* through vigorous averaging[33]. Therefore, in order to discern the stimulus response properties of individual pyramidal cell synapses, it is necessary to record activity further up the dendritic tree by combining electrophysiology with multiphoton imaging techniques.

Sensory tuning at single neocortical synapses. Calcium signals that are measured via multiphoton imaging in pyramidal cell spines provide an indication of how cortical synapses interact during sensory activation[34–36]. An external stimulus can evoke the influx of calcium ions in single cortical spines, and the characteristics of these responses strongly vary between neighbours on the same segment of dendrite. Repeated presentations of the same stimulus can evoke spine calcium responses with high trial-to-trial variability[35] and graded amplitude events (that are prone to failure)[35] or alternatively produce signals with high reliability and minimal variability[35]. Spine-by-spine variations in synaptic transmission, including release probability and postsynaptic receptor density, are likely to account for some of these differences[37]. Calcium signals in spines presumably represent isolated excitatory responses and as such may be used to map the tuning of individual inputs received by the postsynaptic cells.

In primary sensory cortices, the tuning and receptive fields[34–36] of neighbouring synapses are highly heterogeneous (FIG. 2A). In the primary auditory cortex (A1)[35], synapses that display different frequency and bandwidth tuning are colocalized on the same area of the dendrite, and increased stimulus intensity causes the recruitment of increased numbers of spines. In the barrel cortex[34], spines located on the same dendritic branch may preferentially respond to stimulation of

Excitatory postsynaptic currents
Synaptic currents that may be pharmacologically isolated from inhibitory currents recorded in voltage clamp mode and result from the activation of fast glutamatergic receptors.

Horizontal semicircular canals
Fluid-filled tubes that are located in the vestibular organ of the inner ear. Relative movement of fluid within one of the canals corresponds to rotation of the head around the vertical axis.

Stimulus reconstruction
This term describes approaches to calculate approximations of the sensory stimulus based on recorded trains of action potentials or synaptic currents. These can be filters applied to the measured data or Bayesian approaches that determine the most likely stimulus given an observed spike or synaptic current train. These methods help to determine the features in the neuronal data that encode most of the information about the stimulus.

Velocity encoder
A descriptor of a neuron whose synaptic responses most accurately represent velocity rather than acceleration of position of the head during whole-body rotation.

Synaptic receptive fields
The regions of stimulus space in which the presence of a stimulus elicits and/or modulates synaptic activity.

Broadly tuned
Responsiveness to a wide range of stimuli.

Box 1 | **Panoramic subthreshold receptive fields in neocortical cells**

In most cells studied thus far, somatic recordings of postsynaptic potentials (PSPs) in neurons of the barrel cortex[7,8,10,33,39,40,46,54,59], visual cortex[5,12,17,38,41,47–49,52,53,55–58,60,64] and auditory cortex[42–45,50,51,61] reveal cells that have broadly tuned receptive fields. In addition, synaptic activity is evoked by a wide range of stimuli in pyramidal cells of olfactory[150] and multisensory[151] areas. In the barrel cortex (see part **a** of the figure), cells show large synaptic responses to principal whisker (PW) stimulation but also pronounced responses to stimulation of surrounding whiskers (SWs). Whiskers evoking the largest PSPs are most likely to evoke spiking activity[40]. Likewise, in the case of sound location coding in the primary auditory cortex (see part **b** of the figure), individual cells receive synaptic input in response to sound originating from all locations in the frontal hemisphere. Each cell has a preferred location, as defined by the amplitude of the PSP; however, PSPs also show a reliable difference in their rise times. Across the population, contralateral sounds evoke the fastest rates of depolarizations of the excitatory PSP (EPSP) that becomes slower as sound sources are moved into the ipsilateral field, thereby generating additional latency-based information in cortical action potential activity[42].

AP, action potenial; V_m, membrane potential. Part **a** of the figure is adapted, with permission, from REF. 40 © (2003) The Physiological Society. Part **b** of the figure is adapted, with permission, from REF. 42 © (2009) Society for Neuroscience.

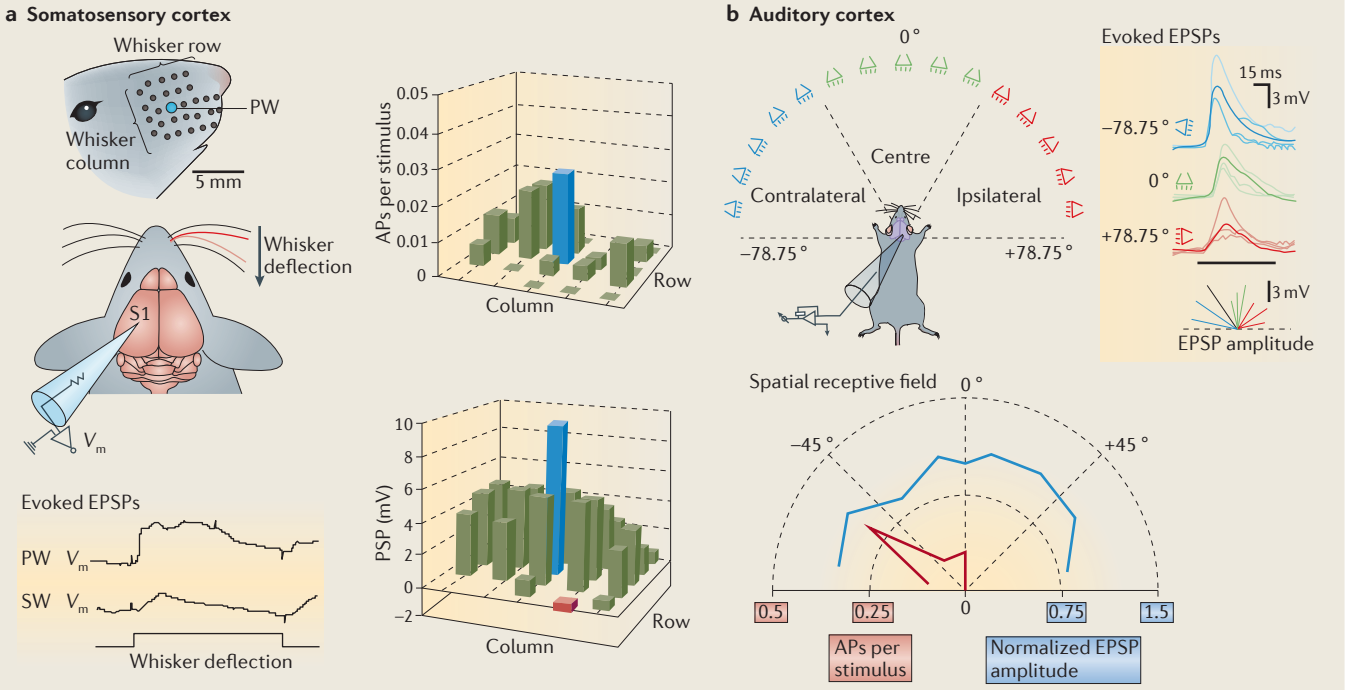

principal and/or surrounding whiskers. Thus, at the local dendritic level, pyramidal cells in the primary sensory neocortex integrate diversely tuned synaptic signals that represent multiple distinct features of the sensory world.

Constructing cellular-scale synaptic representations. Intracellular recordings in pyramidal cells have been widely used to measure stimulus-evoked fluctuations in the subthreshold membrane potential. Such recordings are usually made from the soma, which is close to the final site of integration for synaptic inputs converging across the entire dendritic tree and is an easy target for recording pipettes. Stimulus-driven changes in the amplitude of somatic PSPs are used to construct receptive fields (BOX 1) and measure the overall synaptic tuning of individual cells[1]. Across the neocortex, pyramidal cells have weak preferences for particular stimulus features in their synaptic input, and these result in subthreshold receptive fields that are remarkably broad[5,7,8,10,12,17,38–64]. Indeed, in many cases, receptive fields can be considered 'panoramic': for instance, in the mouse primary visual cortex (V1), synaptic receptive fields show a preference for particular grating orientations, but gratings of any orientation between 0–360 degrees will generate measurable somatic PSPs[12,17,38,41,48,49,60,62–64] (FIG. 2C). Similar schemes are observed in many primary sensory areas: for example, pyramidal cells in area A1 receive panoramic synaptic representations of sound location[42] and show extremely broad subthreshold tuning of sound frequency[44,45,50,51,61]; and tactile stimulation of much of the whisker pad produces PSPs in barrel cortex neurons[7,8,10,39,40,46,54].

These observations confirm that neocortical neurons are afforded a wide view of the sensory world via their synaptic inputs. When taken together with signals that are measured in single spines, it seems to be reasonable to assume that there is very little organization in the distribution of synaptic inputs representing different stimulus features across pyramidal cell dendrites. Sensory-evoked calcium signals at different dendritic locations of the same neuron are more narrowly tuned to stimulus identity than are somatic PSPs[17,36,62–66] in a manner that is similar to the calcium responses that are measured in single spines; therefore, it seems that somatic receptive fields are built up of

Sensory-evoked calcium signals
Changes in calcium levels in dendrites and spines can be measured using fluorescent calcium indicators and serve as a proxy for local electrical activity triggered by a stimulus.

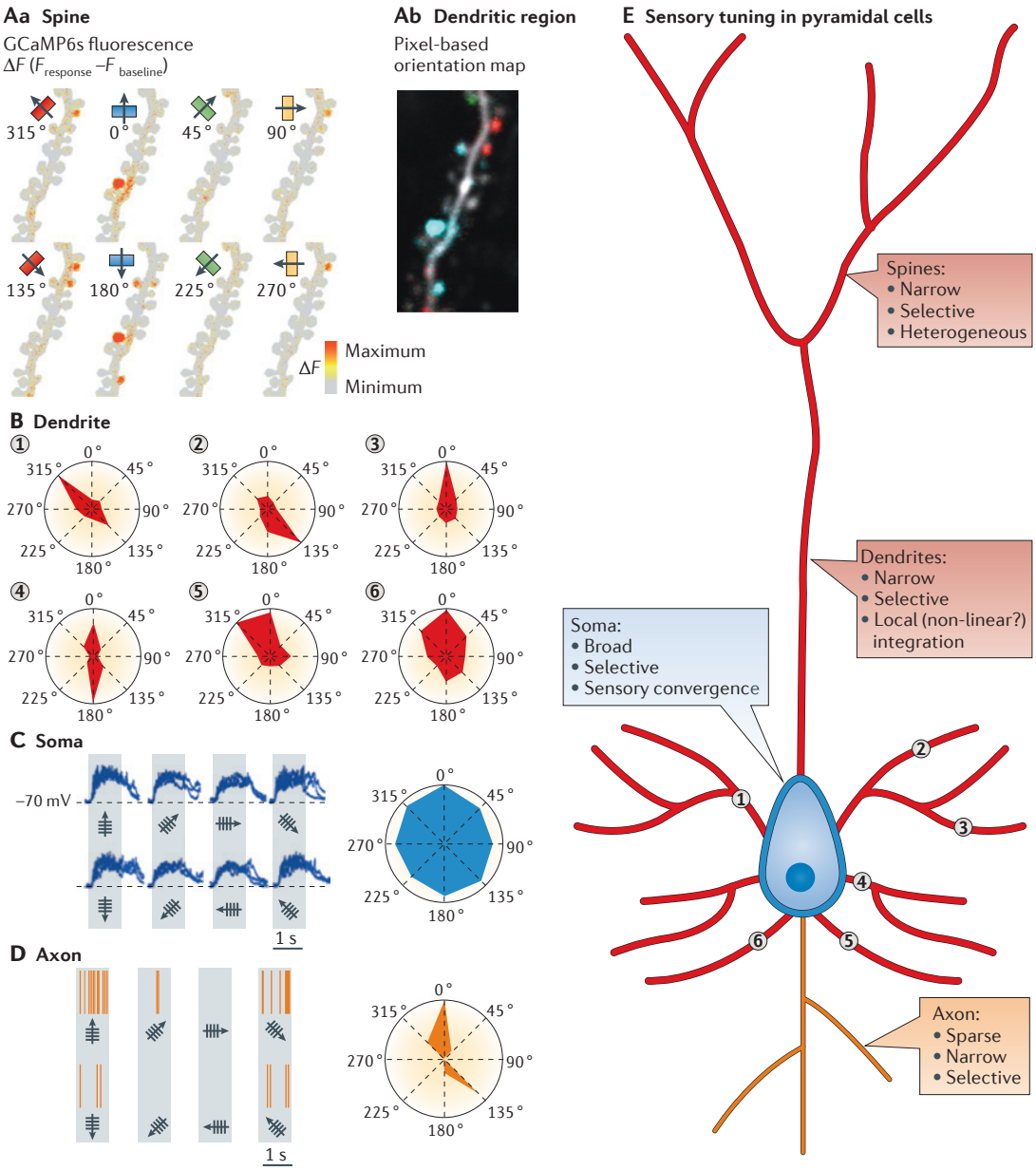

Figure 2 | **Organization and integration of sensory inputs in pyramidal cells.** Combined imaging and electrophysiology reveal postsynaptic activation patterns across pyramidal cells after sensory stimulation. **Aa** | Responses of dendritic spines and neighbouring dendritic shafts of the mouse primary visual cortex pyramidal cells to drifting gratings of different orientations. **Ab** | Adjacent synapses on the same dendritic branch have distinct sensory tuning as revealed by a pixel-based orientation map. **B** | Dendritic 'hotspots' (numbered 1–6) exhibit diverse and narrow sensory tuning profiles. Orientation tuning (measured by changes in intracellular calcium concentration) is very sharp at certain dendritic locations, suggesting local integration of synaptic inputs and the contribution of active dendritic conductances. **C** | At the soma, dendritic subunits converge to generate broad panoramic subthreshold tuning. **D** | The transmission of subthreshold synaptic signals into spike output is restricted to a narrow preferred region of the receptive field. **E** | A summary schematic showing properties of sensory tuning in different compartments of a neocortical pyramidal cell. The numbers correspond to dendritic hotspot locations in panel **B**. Part **A** is reproduced, with permission, from REF. 36 © (2013) Macmillan Publishers Ltd. All rights reserved. Parts **B**–**D** are reproduced, with permission, from REF. 17 © (2010) Macmillan Publishers Ltd. All rights reserved.

Dendritic conductances
Channel-mediated ion flow in dendrites that can boost or attenuate signal propagation.

many stimulus-selective subunits (FIG. 2B). Synaptic integration generates diverse responses at different dendritic locations, a process that is likely to involve both some degree of clustering between co-active synaptic inputs[67] and the contribution of non-linear dendritic conductances[66,68–71].

However, broad synaptic tuning recorded at the soma is typically not reflected in the spike output of the neuron, which is usually sparse and more narrowly tuned (FIG. 2D). Consequently, only a fraction of what a neuron knows about the sensory world is actually reported in

action potential firing. In other words, action potential tuning is the tip of the iceberg of synaptic tuning[41], and the relationship between evoked PSP amplitudes and action potential thresholds is exquisitely balanced. The extent of the synaptic icebergs lurking beneath action potential threshold depends on both neuronal class and topographical location. Layer 5 pyramidal cells express a greater fraction of their synaptic receptive field through action potential output than layer 2/3 neurons[40,46,58]. This laminar difference may in part reflect distinct intrinsic properties or presynaptic connectivity patterns in superficial versus deep-layer pyramidal cells. Neuronal firing rates in layer 5 are generally considerably higher than those in layer 2/3 (REFS 72–75), so cellular excitability may be sufficient to account for the proportion of synaptic responses that are converted into neuronal output. Within layer 5, corticofugal pyramidal neurons exhibit broader synaptic tuning than their corticocortical neighbours[61]. In cat area V1, where neurons are topographically organized with respect to orientation, synaptic receptive fields that are located in areas in which orientation domains converge are markedly broader than those that are located within orientation domains[48,52], suggesting that the local structure of sensory maps also plays a part in the establishing the profile of synaptic receptive fields.

Synaptic dynamics sharpen sensory representations. Neocortical synapses are history-dependent, as they adapt or facilitate their responses to repetitive stimulus presentations[76–80]. Although repeated stimulation is not ubiquitous, it often causes adaptation and a reduction in the amplitude of evoked synaptic excitation in the neocortex[78,81–84], so that during a train of stimuli, the size of evoked PSPs decreases and then stabilizes at low amplitudes (FIG. 3a). Short-term depression of synaptic responsiveness occurs in many regions of the neocortex, persists on the timescale of seconds and is analogous to the synaptic dynamics observed in somatosensory areas of the cerebellar cortex[22].

One consequence of short-term changes in synaptic responsiveness is that the overall profile of synaptic receptive fields during repetitive stimulation can be changed[54,83]. For this reason, receptive field mapping studies have typically used low stimulus presentation rates to avoid history-dependent changes in PSP amplitude confounding the construction of tuning curves. However, behaviourally relevant stimuli are rarely encountered in temporal isolation, so history-dependent changes in synaptic properties may make a marked contribution to active sensory processing. Receptive field mapping using high presentation rates

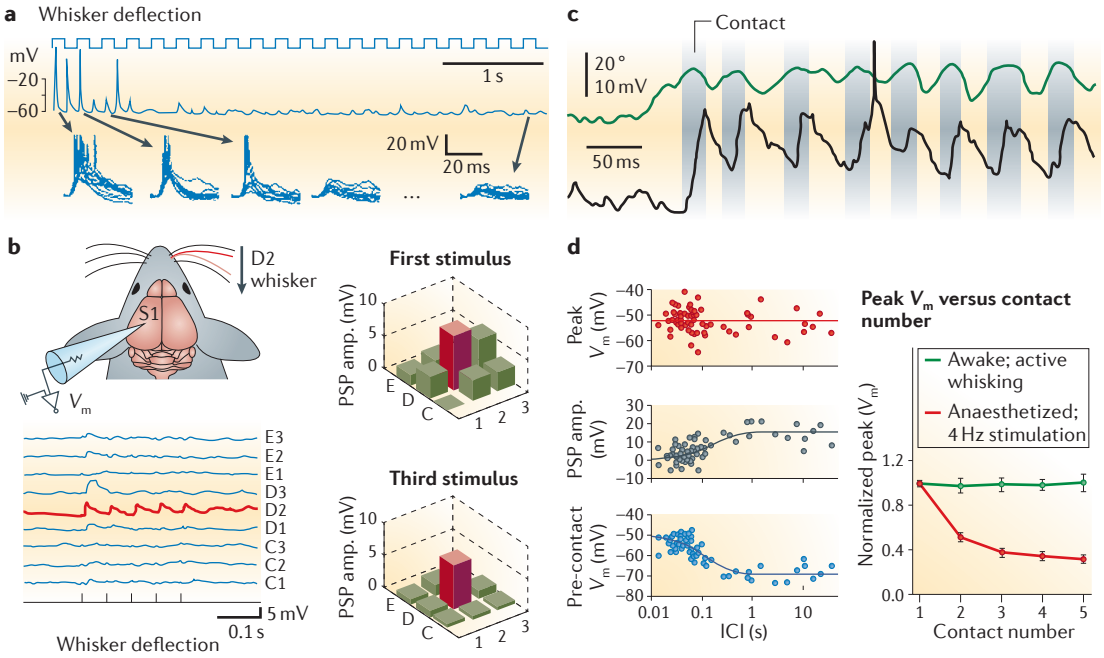

Figure 3 | **Short-term synaptic dynamics tune and sharpen receptive fields.** **a** | Evoked postsynaptic potentials (PSPs) in a barrel cortex cell following 4 Hz stimulation of the principal whisker (PW). PSPs progressively decrease with repetitive stimulation. **b** | The left panel shows the average responses of a barrel cortical neuron to repetitive stimulation of nine different whiskers. The PW (red) shows less adaptation than the other whiskers. The right panel shows the subthreshold receptive fields that are generated for the first and third stimulus in a train. Receptive fields shrink during adaptation. **c** | A whole-cell somatic recording from a barrel cortex pyramidal cell of a head-fixed mouse during active whisking. Whisker contact (in grey) is associated with reliable fluctuations in the membrane potential (V_m). **d** | The amplitude of individual evoked PSPs (middle left trace) depends on the pre-contact V_m (left bottom trace), but the peak membrane potential following object contact is remarkably stable and independent of the intercontact interval (ICI) (top left and right traces). Part **a** is reproduced, with permission, from REF. 82 © (2002) Elsevier. Part **b** is reproduced, with permission, from REF. 54 © (2006) Society for Neuroscience. Parts **c** and **d** are reproduced, with permission, from REF. 85 © (2011) Elsevier.

Orientation domains
In the visual cortex — for example, of cats — orientation preference varies gradually across the cortical surface, resulting in local regions ('domains') in which neurons with a similar orientation preference are grouped together.

shows that synaptic depression has important functional consequences for the representation of sensory events. An overall reduction in the responsiveness of cortical synapses means that synaptic receptive fields are narrower during high presentation rates and that subthreshold tuning is sharper than otherwise observed[54] (FIG. 3b). Therefore, individual neurons are conferred with a broad sensitivity to novel sensory stimulation through their synaptic inputs, but history-dependent changes in synaptic properties may serve to functionally silence most of these inputs *in vivo* during ongoing sensory processing.

Somatic recordings of the membrane potential in awake behaving animals indicate that sensory stimulation actually evokes PSPs that have a robust, reliable amplitude. Active whisker deflections generate unique stereotyped somatic membrane potential fluctuations in individual barrel cortex layer 2/3 neurons[85] (FIG. 3c). The effect of whisker stimulation is to briefly clamp the membrane potential at a fixed voltage, at a value that can be considered the 'whisker-evoked reversal potential' (REFS 85,86). This value typically lies somewhere below the threshold and is established by the sum of excitatory and inhibitory conductances. Thus, if the preceding membrane potential is hyperpolarized relative to the whisker-evoked reversal potential, then stimulation evokes depolarization, whereas if the membrane potential is more depolarized relative to the whisker-evoked reversal potential, then stimulation generates hyperpolarization (FIG. 3d, left). Strikingly, during repetitive whisking, the whisker-evoked reversal potential remains constant, so successive contacts with a stimulus drive the cells to the same final membrane potential[85] (FIG. 3d, right). Synaptic dynamics are therefore at steady-state during periods of active sensory processing, favouring stable representations of sensory signals[86]. And like velocity signalling in cerebellar granule cells, neocortical synaptic representations become more reliable and insensitive to the temporal frequency of the stimulus.

Evoked excitation versus inhibition

Sensory stimulation activates both excitatory and inhibitory elements within the cortex. The manipulation of the membrane potential during intracellular recording has been widely used *in vivo* to segregate excitatory and inhibitory inputs owing to their differing ionic reversal potentials[2,7,12,38,43,49,50,52,83,87–100] (but see also BOX 2). Use of this procedure has led to the conclusion that excitation and inhibition measured at the soma share similar tuning profiles, such that the stimulus that elicits the strongest excitatory synaptic current also evokes the largest inhibitory current. This observation was first made in area V1, where the orientation tuning of excitatory and inhibitory PSPs is similar within individual cells[2]. Similar observations have since been made using voltage and current clamp recordings in other areas of the neocortex, which suggest that excitatory and inhibitory synaptic inputs evoked by, for example, visual stimuli[2,12,38,49,52,88,89,101], sound stimuli[43,50,90–92] and touch stimuli[7,83,93–95] are thought to share similar tuning profiles (FIG. 4a).

Dual intracellular recordings from pairs of neurons *in vivo* demonstrate that synaptic dynamics are highly correlated across cortical networks[95,102–105]. By depolarizing one neuron and simultaneously hyperpolarizing the other, it can be observed that fluctuations in the amplitude of excitatory PSPs in one cell are tracked by inhibitory PSPs in the other on a moment-by-moment basis[95] (FIG. 4b). As the interaction between the opposing forces of excitation and inhibition underlies much, if not all, neuronal computation, it is perhaps surprising that excitatory and inhibitory signals track each other so faithfully in the neocortex.

Following sensory stimulation, pyramidal neurons rarely receive excitatory input without concurrent inhibition (although nucleus basalis stimulation can induce a transient loss of synaptic inhibition[44]). However, there are a number of instances in which inhibition seemingly cancels out excitatory synaptic signals after stimulation. In the auditory cortex, the frequency tuning of synaptic inhibition is slightly broader than that of synaptic excitation, which causes inhibition to dominate the edges of tone receptive fields and produce an overall sharpening of action potential tuning that is analogous to classical lateral inhibition[96]. A subset of A1 neurons also exhibit intensity tuning[97,98], and in these cells inhibition dominates at high sound levels, leading to non-monotonic action potential tuning. In the olfactory cortex, excitatory synaptic input is narrowly tuned and odour-specific, whereas inhibitory synaptic input is globally tuned and invariant to odour identity[99].

These observations imply that although sensory stimulation generally activates a barrage of excitatory and inhibitory synaptic inputs, inhibition can also serve to sharpen recurrent excitation in cortical circuits, and the overall prominence of inhibitory inputs in certain circumstances[99,100,106,107] may be relevant in enforcing the network sparseness that is observed in both the anaesthetized and awake neocortex[100]. Although there is no doubt that such evoked responses result from the interplay between excitatory and inhibitory synaptic activity distributed across the soma–dendritic axis, recent attempts to quantify such interactions on the basis of *in vivo* somatic current injections or voltage clamp recordings seem to be of limited use: the lack of voltage control over the extensive dendritic tree prohibits a straightforward separation of excitatory and inhibitory currents, as estimation of the inhibition/excitation ratio cannot be accurate without knowing the spatial distribution and strength of the underlying synapses (BOX 2). As a result, we have only limited knowledge of the fine-scale interactions between synaptic excitation and inhibition (for instance, at the level of cortical spines[108]) during sensory signalling.

Delayed inhibition reduces firing and promotes asynchrony. Although the tuning of sensory-evoked excitation and inhibition are often well matched, a small temporal delay exists between the two signals[7,90,93,95] (FIG. 4c). For a given stimulus, a characteristic sequence of events is seen in pyramidal cells: activation of excitatory inputs is followed a few milliseconds later by activation

Box 2 | **Estimating excitation and inhibition using voltage clamp *in vivo***

Somatic voltage clamp (VC) has been used to isolate synaptic excitation and inhibition *in vivo*. The rationale being that, at least for isopotential cells, clamping the membrane potential (V_m) at the reversal potential of synaptic excitation (approximately 0 mV) would reduce the driving force for excitation (and thus the excitatory current) to zero, thereby isolating the inhibitory currents to be recorded. Conversely, clamping at the reversal potential of synaptic inhibition (typically around −70 mV) would isolate the excitatory component.

However, even under 'brain silent' conditions, voltage control cannot be achieved substantially beyond the soma owing to the lack of 'space clamp' (REFS 152–155). This has been directly verified using triple recordings from the soma and dendrites[156,157] by injecting a known 'synaptic' conductance at different dendritic locations[158,159]. The local voltage at synapses 100–200 µm from the soma was barely affected by somatic VC. Consequently, the measured somatic excitatory postsynaptic current (EPSC) reflects only a small fraction of the injected synaptic current (see parts **a**,**b** of the figure).

In the presence of dendritic excitatory and inhibitory synaptic activity, both synaptic currents are drastically underestimated, and unclamped inhibition can further reduce EPSCs to the point at which estimates of the excitatory conductance can approach and even, absurdly, fall below zero. Thus, depending on synaptic location and the actual ratio between excitation and inhibition, the estimated ratio (from the somatic VC data) can fall anywhere along a continuum between being under- to overestimated. The left and middle panels of part **c** show actual dendritic conductances (open) and the estimates based on the somatic VC (solid) for injections at varying distances from the soma; the left panel shows excitatory (Exc) conductances and the middle panel shows inhibitory (Inh) conductances. The right panel of part **c** shows the actual (open) and estimated (solid) ratio between excitation and inhibition. These data, together with theoretical studies[154,160], demonstrate that even in a reduced preparation it is not possible to estimate the ratio of synaptic excitation and inhibition without making assumptions about the locations and strengths of the underlying synaptic contacts.

Dendritic synaptic activity *in vivo* is generally increased compared to recordings in brain slices[156], which increases VC error. Compared with anaesthetized preparations, V_m in awake animals is typically more depolarized[126], leading to and resulting from increased dendritic conductances. As a result, estimation and comparison of synaptic conductance ratios across different regimes of network activity[105] is perhaps the most challenging scenario of all, as linear arithmetic will inevitably fail to recover even relative current or conductance amplitude ratios.

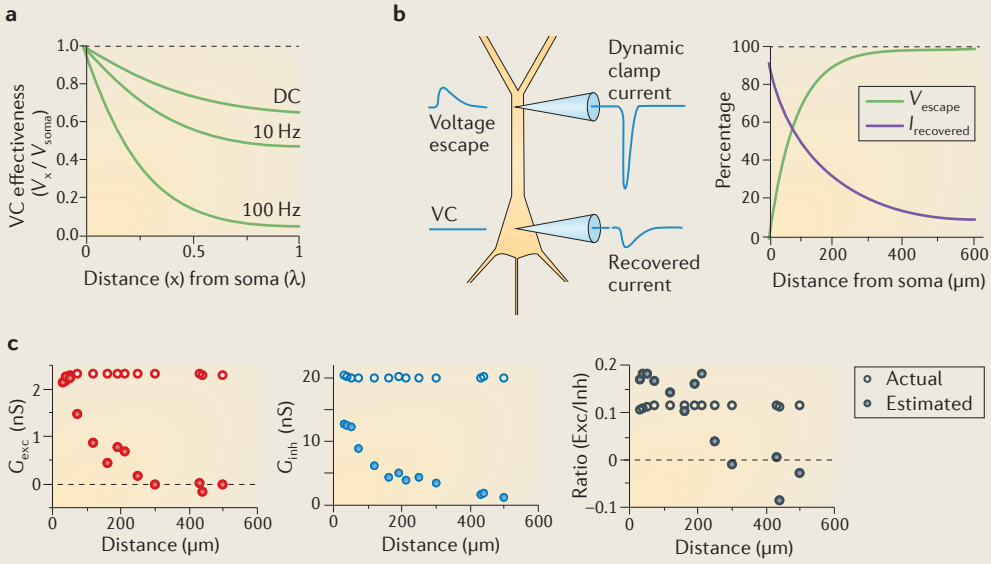

of inhibitory inputs. A straightforward interpretation is that this is a hard-wired delay that provides feedforward inhibition, which serves to greatly reduce the time window during which action potential firing can occur after exposure to a stimulus[109,110].

Theoretical work suggests that balanced synaptic excitation and inhibition is an emergent property of recurrently connected networks, in which populations of excitatory and inhibitory neurons accurately track each other's activity[111]. The consequences of this interplay for sensory processing are several-fold. Neuronal firing rates in response to sensory stimuli are reduced via dampening of network excitation[15]. The temporal reliability of sensory signalling is also improved by drastically restricting the time window of evoked action potential firing[90]. The gain of synaptic integration, which is necessary to maintain sensitivity to the broadest range of input patterns, is partially normalized via instantaneous matching of excitatory and inhibitory amplitudes[112].

Finally, spiking correlations between neurons are kept low within local circuits[111,113–115]. Membrane potential dynamics are correlated across the cortical networks[95,102–105]; overlapping patterns of synaptic input ought to cause highly correlated patterns in the timing of spiking output. Within the recurrently interconnected circuits of the neocortex, such a scheme favours hypersynchronous network activity. Hypersynchrony is not observed, however, under normal conditions. Instead, neurons fire independently of one another following activation, promoting efficient population coding[111,114]. Therefore, one of the most important functions of balanced excitation–inhibition may be to minimize spurious output correlations within networks of neurons that receive overlapping patterns of sensory input. By restricting neuronal excitability[15], limiting the timing of action potential firing[90,93] and promoting network asynchrony[111,113,114], mixed excitatory and inhibitory synaptic inputs preserve the sensitivity of the cortex

Hypersynchronous network activity
The state of (often unnaturally) high synchrony between large populations of neurons, particularly in epileptic discharges, during which extensive groups of neurons simultaneously fire action potentials within a few milliseconds.

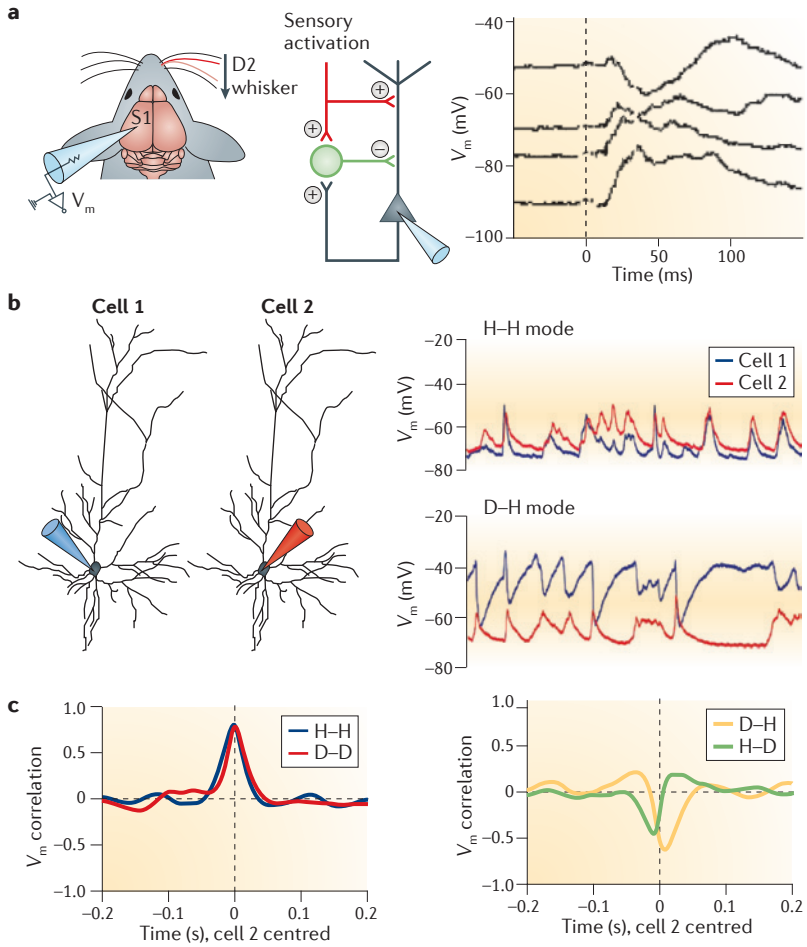

Figure 4 | **Sensory responses result from co-activation of temporally offset excitatory and inhibitory inputs.** **a** | Whisker-evoked postsynaptic potentials (PSPs) recorded in the barrel cortex (left panel) at different membrane potentials (V_m) reveal their mixed excitatory and inhibitory nature owing to feedforward and feedback inhibition onto pyramidal cells (middle panel). At hyperpolarized potentials, excitatory PSPs are visible, whereas at depolarized potentials, the same whisker deflection evokes an inhibitory PSP (right panel). **b** | Simultaneous intracellular recording from two barrel cortex neurons reveal V_m fluctuations to be highly correlated between individual cells. When both neurons are hyperpolarized (H–H), correlated synaptic excitation is observed (top right panel). When one neuron is depolarized (D–H), the correlation between inhibition and excitation can be observed (bottom right panel). **c** | Excitation and inhibition are temporally offset. Cross correlation of V_m between cells reveals that excitation is correlated with zero time delay (left panel), but excitation precedes inhibition by a few milliseconds (right panel). Part **a** is reproduced, with permission, from REF. 7 © (1998) American Physiological Society. Parts **b** and **c** are reproduced, with permission, from REF. 95 © (2008) Macmillan Publishers Ltd. All rights reserved.

to stimuli across various conditions and maximize the number of distinct patterns that can be represented within cortical circuits.

Synaptic integration and ongoing rhythms

Ongoing brain rhythms shape patterns of sensory-evoked input and improve the precision and coding capacity of synaptic representation[116–120]. Different behavioural states are associated with various oscillatory rhythms in cortical circuits, all of which exert their own influence over cortical synaptic signalling.

Synaptic signalling during slow oscillations and cortical desynchronization. During anaesthesia and sleep, network activity in the neocortex is dominated by a slow (1 Hz) oscillation[121]. Within individual neurons, slow oscillations are characterized by periods of steady-state hyperpolarized membrane potential (down states) interleaved with depolarized periods (up states)[95,122–124]. Network and synaptic activity is largely confined to up-state periods[124]. The prominence of the slow oscillation in governing patterns of cortical activity is reflected by differences in the sensory-evoked synaptic signals between the up and down states. Whisker deflections during down states generate reliable large-amplitude depolarizations, whereas deflections during up states are smaller and more variable[122]. During sleep and anaesthesia, sensory activation may only be capable of modulating the occurrence of up states[123] but not of abolishing down states, so even the membrane potential response to sustained sensory stimulation is terminated after a few hundred milliseconds.

Slow oscillations may be useful for consolidating behaviourally relevant patterns of activity (for example, memory consolidation during sleep[125]) and may in some instances aid temporal representations. However, under appropriate conditions, global neocortical activity exhibits a persistent up-like state, which is characterized by fast ongoing fluctuations in the membrane potential[64,103,105,126–129]. This up-like state is known as the activated or desynchronized state, and it is a feature of the neocortex in behaving animals during periods such as active whisking[105,129] (but also occurs spontaneously and sporadically under anaesthesia[111]). In the activated state, the membrane potential is slightly more depolarized[64,126,130] than normal, but despite this change neuronal firing rates do not necessarily increase[10,105,126], including during active sensory behaviours such as whisking[105]. Thus, the conversion of synaptic input into action potential firing remains a rare and exceptional event even in the active neocortex.

Input ramps during theta oscillations in the entorhinal cortex. The functional interaction of network rhythms and sensory-evoked synaptic input is effectively demonstrated in neurons of the medial entorhinal cortex. Grid cells in the medial entorhinal cortex exhibit a striking modulation of their firing rates during navigation according to an environmental map composed of regular triangular lattices[131]. During navigation, the timing of action potential firing is dependent on the theta oscillation, which is present in the medial entorhinal cortex and hippocampus during locomotion. It has been proposed that spatial maps in grid cells could result from interference patterns of theta-frequency oscillatory synaptic input of differing frequencies[132,133]. However, subthreshold grid cell-like responses are also characterized by depolarizing ramps of voltage at regular intervals in space[134,135]. The profiles of these ramps cannot be accounted for through oscillatory interference and instead reflect the summation of synaptic potentials that are evoked by modulations of the presynaptic firing rate that is generated as animals move through space. Therefore, despite strong ongoing theta oscillations, individual neurons integrate synaptic inputs across several theta cycles during field crossings.

In addition, analogously to the synaptic representation of velocity signals in tiny cerebellar granule cells[23], this transformation can be linear, whereby modulations in the rate of excitatory synaptic input provide an accurate readout of navigational space in neurons of the medial entorhinal cortex[134,135]. Theta oscillations therefore regulate precise action potential timing[117], but sustained depolarizations are a hallmark of the subthreshold representation of navigational space.

Active mechanisms shape synaptic integration

Sensory representations in pyramidal cells are formed from overlapping populations of excitatory and inhibitory synapses. Unitary synaptic events are very small[33], may be spread across an extensive dendritic tree[34,35,136] and are subject to network rhythms. Together, this could present a precarious environment in which to reliably encode sensory information.

Until now we have not considered how synaptically driven depolarizations in spines are transmitted to the soma. In the simplest scenario, electrical signals spread passively via dendrites. For small electrotonically compact neurons such as cerebellar granule cells, passive spread of PSPs is little influenced by their size and shape, but in pyramidal cells synaptic signals are prone to substantial filtering and attenuation within dendrites, potentially minimizing their impact at the soma[137]. The extent of this effect has been highlighted in recordings from pyramidal cells in hippocampal area CA1 (REFS 138–140). Two classes of subthreshold membrane potential profile are seen in these cells when recordings are made from maze-running rats and mice. The first population exhibits subthreshold place fields, which are visible as depolarizing voltage ramps[138–140], whereas the second population shows no modulations in the membrane potential during place field traversals[138]. Intriguingly, injection of a depolarizing somatic current in these 'silent' cells is sufficient to instate subthreshold place fields[140]. This result has two important implications: first, pyramidal cells that lack somatic subthreshold place fields still receive navigationally tuned synaptic inputs during maze exploration. Second, the propagation of synaptic

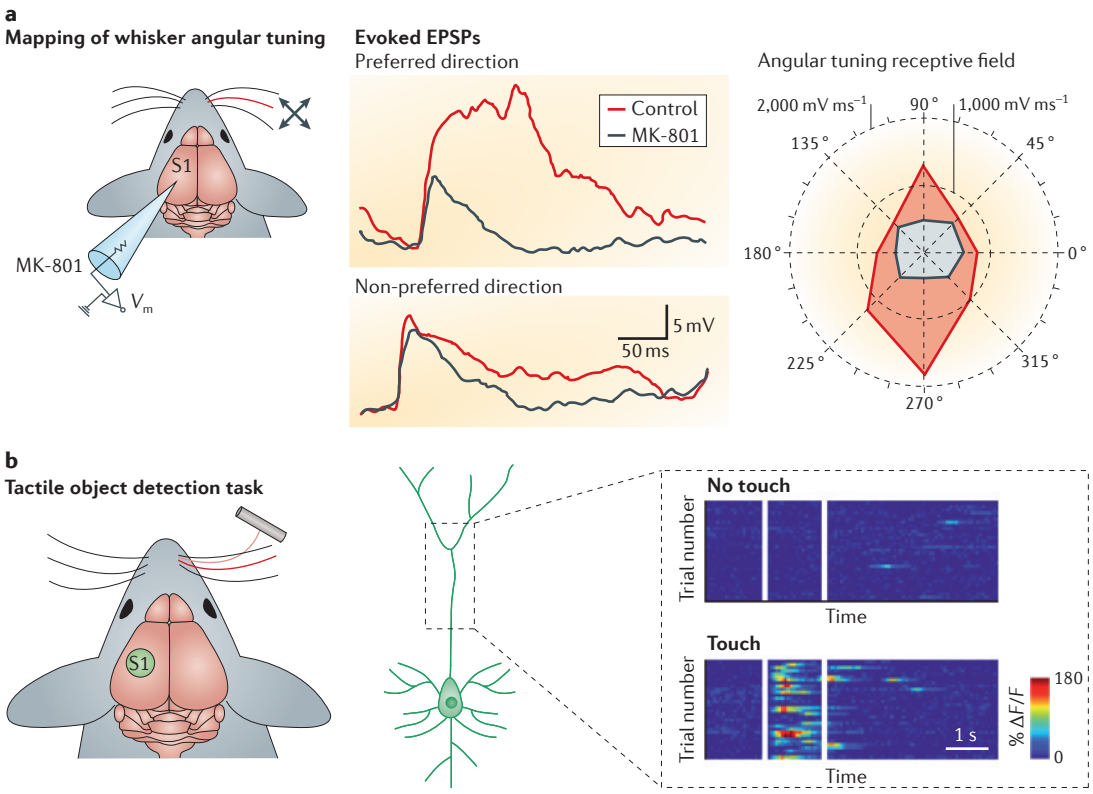

Figure 5 | **Active dendritic conductances in pyramidal cells of awake behaving animals.** **a** | In the barrel cortex, NMDA conductances contribute to the profile of synaptic receptive fields. Mapping of angular tuning of individual whisker-evoked excitatory postsynaptic potentials (EPSPs) in single layer 4 neurons of anaesthetized rats (left) reveals mean whisker-evoked PSPs to preferred (upper traces in the middle panel) and non-preferred (lower traces in the middle panel) movement directions, during control recordings and after intracellular perfusion with MK-801, an NMDA antagonist. The polar plot on the right shows the angular tuning receptive field of the EPSP area obtained 2–8 min (red) and 30–36 min (grey) after whole-cell break-in with an electrode containing MK-801. **b** | Two-photon calcium imaging from layer 5 dendrites in the barrel cortex in mice performing an object detection task. When active contact is made with an object using the principal whisker, calcium spikes are observed in pyramidal cell dendrites (fluorescence change measured as $\Delta F/F$). V_m, membrane potential. Part **a** is reproduced, with permission, from REF. 59 © (2012) Macmillan Publishers Ltd. All rights reserved. Part **b** is reproduced, with permission, from REF. 143 © (2012) Macmillan Publishers Ltd. All rights reserved.

Electrotonically
The term refers to the voltage spread (largely voltage attenuation) along branched structures such as dendrites that is mediated by the 'passive' cellular properties: membrane resistance, membrane capacitance and axial resistance. It can be quantitatively described using cable theory.

signals to the soma is gated within pyramidal cell dendrites. Activation of voltage-dependent conductances — in this case, via artificial current injections — can be crucial for the cellular representation of the sensory environment.

Experimental work in brain slices has revealed a rich variety of mechanisms by which pyramidal cell dendrites can modulate synaptic signals[69,70]. More recently, *in vivo* evidence supports a role for active conductances in the formation of sensory representations. And although certain mechanisms may be in operation in the neurons of anaesthetized animals, there is further evidence that active dendritic processes are particularly prominent in awake behaving animals.

Postsynaptic NMDA receptors have a role in shaping the synaptic receptive fields in area V1 (REF. 66) and the barrel cortex[59]. In layer 4 spiny stellate neurons, intracellular blockade of NMDA receptors reduces both the amplitude and directional tuning of whisker-evoked PSPs, which suggests that the NMDA spikes selectively amplify synaptic responses in preferred regions of the receptive field[59] (FIG. 5a). Sensory-evoked calcium signals have been imaged directly in the distal dendrites of pyramidal neurons *in vivo*[17,66,36,141–143]. In layer 5, dendritic calcium events encode sensory stimulation in a graded manner, in part owing to inhibitory regulation of the size and spatial spread of such signals[141,142]. Global calcium signals are evoked by object touch during periods of active whisking[143], suggesting that calcium spikes are gated by the behavioural state of the animal and are highly relevant to active sensory processing (FIG. 5b). These results highlight that active signalling in pyramidal cell dendrites is a prominent feature of sensory processing in the neocortex and furthermore suggest that active sensing gives rise to active dendritic conductances.

Outlook and conclusions

The challenges involved in monitoring sensory signalling *in vivo* and the inherent limitations of somatic recordings in large neurons mean that we still have much to learn about how these processes contribute to the synaptic representation of active sensation. In particular, the functional tuning of active conductances in neurons and the role of inhibition in gating synaptic integration in spines and dendrites remain rich fields for study. *In vivo* whole-cell recordings combined with single-cell transfection of the recorded neuron[53] and new tools for mapping the distribution of synapses[136,144] are very likely to provide a more complete picture of the functional organization of synaptic connectivity onto single cells and cortical circuits in general.

Recent advances in *in vivo* intracellular recordings have enabled us to gain increasing insight into the nature of the subthreshold events that underlie evoked action potential discharge in anaesthetized and awake preparations. They also offer the opportunity to unravel the intricacies of the interplay between inhibitory and excitatory synaptic inputs. Although a pure electrophysiological approach to separating inhibition and excitation suffers from the lack of adequate voltage control over the dendritic tree, strategies in which electrophysiology is complemented by imaging as well as detailed knowledge of synapse distribution and comprehensive computational modelling are beginning to emerge. New experimental tools — for example, including three-dimensional serial microscopy[145,146] and rapid multiphoton imaging[147–149] — could better constrain such data analysis and provide novel insights into the cellular and subcellular interactions between excitatory and inhibitory synaptic inputs *in vivo*. However, recordings of evoked synaptic activity have already highlighted the inherent diversity and flexibility of sensory signalling within pyramidal cells.

1. Creutzfeldt, O. & Ito, M. Functional synaptic organization of primary visual cortex neurones in the cat. *Exp. Brain Res.* **6**, 324–352 (1968).
2. Ferster, D. Orientation selectivity of synaptic potentials in neurons of cat primary visual cortex. *J. Neurosci.* **6**, 1284–1301 (1986).
3. Carvell, G. E. & Simons, D. J. Membrane potential changes in rat SmI cortical neurons evoked by controlled stimulation of mystacial vibrissae. *Brain Res.* **448**, 186–191 (1988).
4. Pei, X., Volgushev, M., Vidyasagar, T. R. & Creutzfeldt, O. D. Whole cell recording and conductance measurements in cat visual cortex *in-vivo*. *Neuroreport* **2**, 485–488 (1991).
5. Jagadeesh, B., Wheat, H. S. & Ferster, D. Linearity of summation of synaptic potentials underlying direction selectivity in simple cells of the cat visual cortex. *Science* **262**, 1901–1904 (1993).
6. Covey, E., Kauer, J. A. & Casseday, J. H. Whole-cell patch-clamp recording reveals subthreshold sound-evoked postsynaptic currents in the inferior colliculus of awake bats. *J. Neurosci.* **16**, 3009–3018 (1996).
7. Moore, C. I. & Nelson, S. B. Spatio-temporal subthreshold receptive fields in the vibrissa representation of rat primary somatosensory cortex. *J. Neurophysiol.* **80**, 2882–2892 (1998).
8. Zhu, J. J. & Connors, B. W. Intrinsic firing patterns and whisker-evoked synaptic responses of neurons in the rat barrel cortex. *J. Neurophysiol.* **81**, 1171–1183 (1999).
9. Fee, M. S. Active stabilization of electrodes for intracellular recording in awake behaving animals. *Neuron* **27**, 461–468 (2000).
10. Margrie, T. W., Brecht, M. & Sakmann, B. *In vivo*, low-resistance, whole-cell recordings from neurons in the anaesthetized and awake mammalian brain. *Pflugers Arch.* **444**, 491–498 (2002).
In this article, the authors suggest that there is sparse coding in the cortex on the basis of their observation that *in vivo* whole-cell recordings show low spontaneous and sensory-evoked firing rates.
11. Margrie, T. W. *et al.* Targeted whole-cell recordings in the mammalian brain *in vivo*. *Neuron* **39**, 911–918 (2003).
12. Monier, C., Chavane, F., Baudot, P., Graham, L. J. & Frégnac, Y. Orientation and direction selectivity of synaptic inputs in visual cortical neurons: a diversity of combinations produces spike tuning. *Neuron* **37**, 663–680 (2003).
13. Dittgen, T. *et al.* Lentivirus-based genetic manipulations of cortical neurons and their optical and electrophysiological monitoring *in vivo*. *Proc. Natl Acad. Sci. USA* **101**, 18206–18211 (2004).
14. Kitamura, K., Judkewitz, B., Kano, M., Denk, W. & Häusser, M. Targeted patch-clamp recordings and single-cell electroporation of unlabeled neurons *in vivo*. *Nature Methods* **5**, 61–67 (2008).
15. Gentet, L. J., Avermann, M., Matyas, F., Staiger, J. F. & Petersen, C. C. H. Membrane potential dynamics of GABAergic neurons in the barrel cortex of behaving mice. *Neuron* **65**, 422–435 (2010).
16. Gentet, L. J. *et al.* Unique functional properties of somatostatin-expressing GABAergic neurons in mouse barrel cortex. *Nature Neurosci.* **15**, 607–612 (2012).
17. Jia, H., Rochefort, N. L., Chen, X. & Konnerth, A. Dendritic organization of sensory input to cortical neurons *in vivo*. *Nature* **464**, 1307–1312 (2010).
In this study, the authors record visually evoked calcium signals in different dendritic regions of the same neuron. They show that different dendrites exhibit highly distinct sensory tuning and that the soma of a single neuron integrates the signals of many distinct functional subunits.
18. Jakab, R. L. & Hámori, J. Quantitative morphology and synaptology of cerebellar glomeruli in the rat. *Anat. Embryol.* **179**, 81–88 (1988).
19. Silver, R. A., Traynelis, S. F. & Cull-Candy, S. G. Rapid-time-course miniature and evoked excitatory currents at cerebellar synapses *in situ*. *Nature* **355**, 163–166 (1992).
20. Chadderton, P., Margrie, T. W. & Häusser, M. Integration of quanta in cerebellar granule cells during sensory processing. *Nature* **428**, 856–860 (2004).
21. Jörntell, H. & Ekerot, C.-F. Properties of somatosensory synaptic integration in cerebellar granule cells *in vivo*. *J. Neurosci.* **26**, 11786–11797 (2006).
22. Rancz, E. A. *et al.* High-fidelity transmission of sensory information by single cerebellar mossy fibre boutons. *Nature* **450**, 1245–1248 (2007).

23. Arenz, A., Silver, R. A., Schaefer, A. T. & Margrie, T. W. The contribution of single synapses to sensory representation *in vivo*. *Science* **321**, 977–980 (2008).
In this study, the authors directly measure the contribution of individual synaptic inputs to the representation of velocity signals in cerebellar granule cells.
24. Bengtsson, F. & Jörntell, H. Sensory transmission in cerebellar granule cells relies on similarly coded mossy fiber inputs. *Proc. Natl Acad. Sci. USA* **106**, 2389–2394 (2009).
25. Sawtell, N. B. Multimodal integration in granule cells as a basis for associative plasticity and sensory prediction in a cerebellum-like circuit. *Neuron* **66**, 573–584 (2010).
The author demonstrates that multimodal synaptic integration underlies action potential output in granule cells of electric fish.
26. Duguid, I., Branco, T., London, M., Chadderton, P. & Häusser, M. Tonic inhibition enhances fidelity of sensory information transmission in the cerebellar cortex. *J. Neurosci.* **32**, 11132–11143 (2012).
27. Huang, C.-C. *et al.* Convergence of pontine and proprioceptive streams onto multimodal cerebellar granule cells. *eLife* **2**, e00400 (2013).
28. Albus, J. S. A theory of cerebellar function. *Math. Biosci.* **10**, 25–61 (1971).
29. Marr, D. A theory of cerebellar cortex. *J. Physiol. (Lond.)* **202**, 437–470 (1969).
30. Schweighofer, N., Doya, K. & Lay, F. Unsupervised learning of granule cell sparse codes enhances cerebellar adaptive control. *Neuroscience* **103**, 35–50 (2001).
31. Tyrrell, T. & Willshaw, D. Cerebellar cortex: its simulation and the relevance of Marr's theory. *Phil. Trans. R. Soc. Lond. B* **336**, 239–257 (1992).
32. Spruston, N. Pyramidal neurons: dendritic structure and synaptic integration. *Nature Rev. Neurosci.* **9**, 206–221 (2008).
33. Bruno, R. M. & Sakmann, B. Cortex is driven by weak but synchronously active thalamocortical synapses. *Science* **312**, 1622–1627 (2006).
34. Varga, Z., Jia, H., Sakmann, B. & Konnerth, A. Dendritic coding of multiple sensory inputs in single cortical neurons *in vivo*. *Proc. Natl Acad. Sci. USA* **108**, 15420–15425 (2011).
35. Chen, X., Leischner, U., Rochefort, N. L., Nelken, I. & Konnerth, A. Functional mapping of single spines in cortical neurons *in vivo*. *Nature* **475**, 501–505 (2011).
In this study, the authors record evoked calcium signals in single spines of A1 pyramidal cells. They show that neighbouring spines exhibit distinct sensory tuning and thus that sensory integration may occur locally in pyramidal cell dendrites.
36. Chen, T.-W. *et al.* Ultrasensitive fluorescent proteins for imaging neuronal activity. *Nature* **499**, 295–300 (2013).
37. Nimchinsky, E. A., Sabatini, B. L. & Svoboda, K. Structure and function of dendritic spines. *Annu. Rev. Physiol.* **64**, 313–353 (2002).
38. Anderson, J. S., Carandini, M. & Ferster, D. Orientation tuning of input conductance, excitation, and inhibition in cat primary visual cortex. *J. Neurophysiol.* **84**, 909–926 (2000).
39. Brecht, M. & Sakmann, B. Dynamic representation of whisker deflection by synaptic potentials in spiny stellate and pyramidal cells in the barrels and septa of layer 4 rat somatosensory cortex. *J. Physiol. (Lond.)* **543**, 49–70 (2002).
40. Brecht, M., Roth, A. & Sakmann, B. Dynamic receptive fields of reconstructed pyramidal cells in layers 3 and 2 of rat somatosensory barrel cortex. *J. Physiol. (Lond.)* **553**, 243–265 (2003).
41. Carandini, M. & Ferster, D. Membrane potential and firing rate in cat primary visual cortex. *J. Neurosci.* **20**, 470–484 (2000).
42. Chadderton, P., Agapiou, J. P., McAlpine, D. & Margrie, T. W. The synaptic representation of sound source location in auditory cortex. *J. Neurosci.* **29**, 14127–14135 (2009).
43. Ye, C., Poo, M., Dan, Y. & Zhang, X. Synaptic mechanisms of direction selectivity in primary auditory cortex. *J. Neurosci.* **30**, 1861–1868 (2010).
44. Froemke, R. C., Merzenich, M. M. & Schreiner, C. E. A synaptic memory trace for cortical receptive field plasticity. *Nature* **450**, 425–429 (2007).
45. Liu, B., Wu, G. K., Arbuckle, R., Tao, H. W. & Zhang, L. I. Defining cortical frequency tuning with recurrent excitatory circuitry. *Nature Neurosci.* **10**, 1594–1600 (2007).
46. Manns, I. D., Sakmann, B. & Brecht, M. Sub- and suprathreshold receptive field properties of pyramidal neurones in layers 5A and 5B of rat somatosensory barrel cortex. *J. Physiol. (Lond.)* **556**, 601–622 (2004).
47. Pei, X., Vidyasagar, T. R., Volgushev, M. & Creutzfeldt, O. D. Receptive field analysis and orientation selectivity of postsynaptic potentials of simple cells in cat visual cortex. *J. Neurosci.* **14**, 7130–7140 (1994).
48. Schummers, J., Mariño, J. & Sur, M. Synaptic integration by V1 neurons depends on location within the orientation map. *Neuron* **36**, 969–978 (2002).
49. Tan, A. Y. Y., Brown, B. D., Scholl, B., Mohanty, D. & Priebe, N. J. Orientation selectivity of synaptic input to neurons in mouse and cat primary visual cortex. *J. Neurosci.* **31**, 12339–12350 (2011).
50. Tan, A. Y. Y., Zhang, L. I., Merzenich, M. M. & Schreiner, C. E. Tone-evoked excitatory and inhibitory synaptic conductances of primary auditory cortex neurons. *J. Neurophysiol.* **92**, 630–643 (2004).
51. Kaur, S., Lazar, R. & Metherate, R. Intracortical pathways determine breadth of subthreshold frequency receptive fields in primary auditory cortex. *J. Neurophysiol.* **91**, 2551–2567 (2004).
52. Mariño, J. *et al.* Invariant computations in local cortical networks with balanced excitation and inhibition. *Nature Neurosci.* **8**, 194–201 (2005).
53. Rancz, E. A. *et al.* Transfection via whole-cell recording *in vivo*: bridging single-cell physiology, genetics and connectomics. *Nature Neurosci.* **14**, 527–532 (2011).
54. Katz, Y., Heiss, J. E. & Lampl, I. Cross-whisker adaptation of neurons in the rat barrel cortex. *J. Neurosci.* **26**, 13363–13372 (2006).
55. Volgushev, M., Pernberg, J. & Eysel, U. T. Comparison of the selectivity of postsynaptic potentials and spike responses in cat visual cortex. *Eur. J. Neurosci.* **12**, 257–263 (2000).
56. Jagadeesh, B., Wheat, H. S., Kontsevich, L. L., Tyler, C. W. & Ferster, D. Direction selectivity of synaptic potentials in simple cells of the cat visual cortex. *J. Neurophysiol.* **78**, 2772–2789 (1997).
57. Bringuier, V., Chavane, F., Glaeser, L. & Frégnac, Y. Horizontal propagation of visual activity in the synaptic integration field of area 17 neurons. *Science* **283**, 695–699 (1999).
58. Martinez, L. M., Alonso, J.-M., Reid, R. C. & Hirsch, J. A. Laminar processing of stimulus orientation in cat visual cortex. *J. Physiol. (Lond.)* **540**, 321–333 (2002).
59. Lavzin, M., Rapoport, S., Polsky, A., Garion, L. & Schiller, J. Nonlinear dendritic processing determines angular tuning of barrel cortex neurons *in vivo*. *Nature* **490**, 397–401 (2012).
60. Longordo, F., To, M.-S., Ikeda, K. & Stuart, G. J. Sublinear integration underlies binocular processing in primary visual cortex. *Nature Neurosci.* **16**, 714–723 (2013).
61. Sun, Y. J., Kim, Y.-J., Ibrahim, L. A., Tao, H. W. & Zhang, L. I. Synaptic mechanisms underlying functional dichotomy between intrinsic-bursting and regular-spiking neurons in auditory cortical layer 5. *J. Neurosci.* **33**, 5326–5339 (2013).
62. Li, Y.-T., Ibrahim, L. A., Liu, B.-H., Zhang, L. I. & Tao, H. W. Linear transformation of thalamocortical input by intracortical excitation. *Nature Neurosci.* **16**, 1324–1330 (2013).
63. Lien, A. D. & Scanziani, M. Tuned thalamic excitation is amplified by visual cortical circuits. *Nature Neurosci.* **16**, 1315–1323 (2013).
64. Polack, P.-O., Friedman, J. & Golshani, P. Cellular mechanisms of brain state-dependent gain modulation in visual cortex. *Nature Neurosci.* **16**, 1331–1339 (2013).
65. Hill, D. N., Varga, Z., Jia, H., Sakmann, B. & Konnerth, A. Multibranch activity in basal and tuft dendrites during firing of layer 5 cortical neurons *in vivo*. *Proc. Natl Acad. Sci. USA* **110**, 13618–13623 (2013).
66. Smith, S. L., Smith, I. T., Branco, T. & Häusser, M. Dendritic spikes enhance stimulus selectivity in cortical neurons *in vivo*. *Nature* **503**, 115–120 (2013).
67. Takahashi, N. *et al.* Locally synchronized synaptic inputs. *Science* **335**, 353–356 (2012).
68. Larkum, M. E. & Nevian, T. Synaptic clustering by dendritic signalling mechanisms. *Curr. Opin. Neurobiol.* **18**, 321–331 (2008).
69. Johnston, D., Magee, J. C., Colbert, C. M. & Cristie, B. R. Active properties of neuronal dendrites. *Annu. Rev. Neurosci.* **19**, 165–186 (1996).
70. London, M. & Häusser, M. Dendritic computation. *Annu. Rev. Neurosci.* **28**, 503–532 (2005).
71. Häusser, M., Spruston, N. & Stuart, G. J. Diversity and dynamics of dendritic signaling. *Science* **290**, 739–744 (2000).
72. Wilent, W. B. & Contreras, D. Synaptic responses to whisker deflections in rat barrel cortex as a function of cortical layer and stimulus intensity. *J. Neurosci.* **24**, 3985–3998 (2004).
73. De Kock, C. P. J., Bruno, R. M., Spors, H. & Sakmann, B. Layer- and cell-type-specific suprathreshold stimulus representation in rat primary somatosensory cortex. *J. Physiol. (Lond.)* **581**, 139–154 (2007).
74. Wallace, M. N. & Palmer, A. R. Laminar differences in the response properties of cells in the primary auditory cortex. *Exp. Brain Res.* **184**, 179–191 (2008).
75. Sakata, S. & Harris, K. D. Laminar structure of spontaneous and sensory-evoked population activity in auditory cortex. *Neuron* **64**, 404–418 (2009).
76. Zucker, R. S. & Regehr, W. G. Short-term synaptic plasticity. *Annu. Rev. Physiol.* **64**, 355–405 (2002).
77. Silver, R. A. Neuronal arithmetic. *Nature Rev. Neurosci.* **11**, 474–489 (2010).
78. Borst, J. G. G. The low synaptic release probability *in vivo*. *Trends Neurosci.* **33**, 259–266 (2010).
79. Thomson, A. M. Facilitation, augmentation and potentiation at central synapses. *Trends Neurosci.* **23**, 305–312 (2000).
80. Fioravante, D. & Regehr, W. G. Short-term forms of presynaptic plasticity. *Curr. Opin. Neurobiol.* **21**, 269–274 (2011).
81. Wehr, M. & Zador, A. M. Synaptic mechanisms of forward suppression in rat auditory cortex. *Neuron* **47**, 437–445 (2005).
82. Chung, S., Li, X. & Nelson, S. B. Short-term depression at thalamocortical synapses contributes to rapid adaptation of cortical sensory responses *in vivo*. *Neuron* **34**, 437–446 (2002).
83. Heiss, J. E., Katz, Y., Ganmor, E. & Lampl, I. Shift in the balance between excitation and inhibition during sensory adaptation of S1 neurons. *J. Neurosci.* **28**, 13320–13330 (2008).
84. Higley, M. J. & Contreras, D. Frequency adaptation modulates spatial integration of sensory responses in the rat whisker system. *J. Neurophysiol.* **97**, 3819–3824 (2007).
85. Crochet, S., Poulet, J. F. A., Kremer, Y. & Petersen, C. C. H. Synaptic mechanisms underlying sparse coding of active touch. *Neuron* **69**, 1160–1175 (2011).
The authors demonstrate that sensory stimulation during active whisking is associated with reliable, non-depressing membrane potential deflections in layer 2/3 barrel cortex neurons.
86. Sachidhanandam, S. Sreenivasan, V., Kyriakatos, A., Kremer, Y. & Petersen, C. C. H. Membrane potential correlates of sensory perception in mouse barrel cortex. *Nature Neurosci.* **16**, 1671–1677 (2013).
87. Borg-Graham, L. J., Monier, C. & Frégnac, Y. Visual input evokes transient and strong shunting inhibition in visual cortical neurons. *Nature* **393**, 369–373 (1998).
88. Liu, B. *et al.* Broad inhibition sharpens orientation selectivity by expanding input dynamic range in mouse simple cells. *Neuron* **71**, 542–554 (2011).
89. Haider, B. *et al.* Synaptic and network mechanisms of sparse and reliable visual cortical activity during nonclassical receptive field stimulation. *Neuron* **65**, 107–121 (2010).
90. Wehr, M. & Zador, A. M. Balanced inhibition underlies tuning and sharpens spike timing in auditory cortex. *Nature* **426**, 442–446 (2003).
91. Zhang, L. I., Tan, A. Y. Y., Schreiner, C. E. & Merzenich, M. M. Topography and synaptic shaping of direction selectivity in primary auditory cortex. *Nature* **424**, 201–205 (2003).
92. Tan, A. Y. Y. & Wehr, M. Balanced tone-evoked synaptic excitation and inhibition in mouse auditory cortex. *Neuroscience* **163**, 1302–1315 (2009).
93. Wilent, W. B. & Contreras, D. Dynamics of excitation and inhibition underlying stimulus selectivity in rat somatosensory cortex. *Nature Neurosci.* **8**, 1364–1370 (2005).
94. Higley, M. J. & Contreras, D. Balanced excitation and inhibition determine spike timing during frequency adaptation. *J. Neurosci.* **26**, 448–457 (2006).

95. Okun, M. & Lampl, I. Instantaneous correlation of excitation and inhibition during ongoing and sensory-evoked activities. *Nature Neurosci.* **11**, 535–537 (2008).
In this study, the authors use dual intracellular recordings in the barrel cortex to measure the correlation between synaptic excitation and inhibition in the local network directly. Their work reveals that excitation and inhibition are highly correlated but that the two signals are offset by a few milliseconds, a delay that is enforced by feedforward inhibition.
96. Wu, G. K., Arbuckle, R., Liu, B.-H., Tao, H. W. & Zhang, L. I. Lateral sharpening of cortical frequency tuning by approximately balanced inhibition. *Neuron* **58**, 132–143 (2008).
97. Wu, G. K., Li, P., Tao, H. W. & Zhang, L. I. Nonmonotonic synaptic excitation and imbalanced inhibition underlying cortical intensity tuning. *Neuron* **52**, 705–715 (2006).
98. Tan, A. Y. Y., Atencio, C. A., Polley, D. B., Merzenich, M. M. & Schreiner, C. E. Unbalanced synaptic inhibition can create intensity-tuned auditory cortex neurons. *Neuroscience* **146**, 449–462 (2007).
99. Poo, C. & Isaacson, J. S. Odor representations in olfactory cortex: 'sparse' coding, global inhibition, and oscillations. *Neuron* **62**, 850–861 (2009).
100. Haider, B., Häusser, M. & Carandini, M. Inhibition dominates sensory responses in the awake cortex. *Nature* **493**, 97–100 (2013).
101. Bennett, C., Arroyo, S. & Hestrin, S. Subthreshold mechanisms underlying state-dependent modulation of visual responses. *Neuron* **80**, 350–357 (2013).
102. Lampl, I., Reichova, I. & Ferster, D. Synchronous membrane potential fluctuations in neurons of the cat visual cortex. *Neuron* **22**, 361–374 (1999).
103. Hasenstaub, A. *et al.* Inhibitory postsynaptic potentials carry synchronized frequency information in active cortical networks. *Neuron* **47**, 423–435 (2005).
104. Volgushev, M., Chauvette, S., Mukovski, M. & Timofeev, I. Precise long-range synchronization of activity and silence in neocortical neurons during slow-wave oscillations [corrected]. *J. Neurosci.* **26**, 5665–5672 (2006).
105. Poulet, J. F. A. & Petersen, C. C. H. Internal brain state regulates membrane potential synchrony in barrel cortex of behaving mice. *Nature* **454**, 881–885 (2008).
106. Iurilli, G. *et al.* Sound-driven synaptic inhibition in primary visual cortex. *Neuron* **73**, 814–828 (2012).
107. Dilgen, J., Tejeda, H. A. & O'Donnell, P. Amygdala inputs drive feedforward inhibition in the medial prefrontal cortex. *J. Neurophysiol.* **110**, 221–229 (2013).
108. Chiu, C. Q. *et al.* Compartmentalization of GABAergic inhibition by dendritic spines. *Science* **340**, 759–762 (2013).
109. Hirsch, J. A. & Gilbert, C. D. Synaptic physiology of horizontal connections in the cat's visual cortex. *J. Neurosci.* **11**, 1800–1809 (1991).
110. Pouille, F. & Scanziani, M. Enforcement of temporal fidelity in pyramidal cells by somatic feed-forward inhibition. *Science* **293**, 1159–1163 (2001).
111. Renart, A. *et al.* The asynchronous state in cortical circuits. *Science* **327**, 587–590 (2010).
This study uses theoretical modelling and population recording to show that cortical networks can maintain a desynchronized state despite strong and dense recurrent connectivity. Network excitation and inhibition track one another, with the overall effect of reducing correlated firing among neurons receiving similar patterns of synaptic input.
112. Pouille, F., Marin-Burgin, A., Adesnik, H., Atallah, B. V. & Scanziani, M. Input normalization by global feedforward inhibition expands cortical dynamic range. *Nature Neurosci.* **12**, 1577–1585 (2009).
113. Middleton, J. W., Omar, C., Doiron, B. & Simons, D. J. Neural correlation is stimulus modulated by feedforward inhibitory circuitry. *J. Neurosci.* **32**, 506–518 (2012).
114. Ly, C., Middleton, J. W. & Doiron, B. Cellular and circuit mechanisms maintain low spike co-variability and enhance population coding in somatosensory cortex. *Front. Comput. Neurosci.* **6**, 7 (2012).
115. Van Vreeswijk, C. & Sompolinsky, H. Chaos in neuronal networks with balanced excitatory and inhibitory activity. *Science* **274**, 1724–1726 (1996).
116. Singer, W. & Gray, C. M. Visual feature integration and the temporal correlation hypothesis. *Annu. Rev. Neurosci.* **18**, 555–586 (1995).
117. Schaefer, A. T., Angelo, K., Spors, H. & Margrie, T. W. Neuronal oscillations enhance stimulus discrimination by ensuring action potential precision. *PLoS Biol.* **4**, e163 (2006).
118. Engel, T. A., Helbig, B., Russell, D. F., Schimansky-Geier, L. & Neiman, A. B. Coherent stochastic oscillations enhance signal detection in spiking neurons. *Phys. Rev. E Stat. Nonlin. Soft Matter Phys.* **80**, 021919 (2009).
119. Wang, X.-J. Neurophysiological and computational principles of cortical rhythms in cognition. *Physiol. Rev.* **90**, 1195–1268 (2010).
120. Ainsworth, M. *et al.* Rates and rhythms: a synergistic view of frequency and temporal coding in neuronal networks. *Neuron* **75**, 572–583 (2012).
121. Steriade, M., Contreras, D., Curró Dossi, R. & Nuñez, A. The slow (< 1 Hz) oscillation in reticular thalamic and thalamocortical neurons: scenario of sleep rhythm generation in interacting thalamic and neocortical networks. *J. Neurosci.* **13**, 3284–3299 (1993).
122. Petersen, C. C. H., Hahn, T. T. G., Mehta, M., Grinvald, A. & Sakmann, B. Interaction of sensory responses with spontaneous depolarization in layer 2/3 barrel cortex. *Proc. Natl Acad. Sci.* **100**, 13638–13643 (2003).
123. Hasenstaub, A., Sachdev, R. N. S. & McCormick, D. A. State changes rapidly modulate cortical neuronal responsiveness. *J. Neurosci.* **27**, 9607–9622 (2007).
124. Saleem, A. B., Chadderton, P., Apergis-Schoute, J., Harris, K. D. & Schultz, S. R. Methods for predicting cortical UP and DOWN states from the phase of deep layer local field potentials. *J. Comput. Neurosci.* **29**, 49–62 (2010).
125. Rasch, B. & Born, J. About sleep's role in memory. *Physiol. Rev.* **93**, 681–766 (2013).
126. Constantinople, C. M. & Bruno, R. M. Effects and mechanisms of wakefulness on local cortical networks. *Neuron* **69**, 1061–1068 (2011).
127. Steriade, M., Timofeev, I. & Grenier, F. Natural waking and sleep states: a view from inside neocortical neurons. *J. Neurophysiol.* **85**, 1969–1985 (2001).
128. Harris, K. D. & Thiele, A. Cortical state and attention. *Nature Rev. Neurosci.* **12**, 509–523 (2011).
129. Zagha, E., Casale, A. E., Sachdev, R. N. S., McGinley, M. J. & McCormick, D. A. Motor cortex feedback influences sensory processing by modulating network state. *Neuron* **79**, 567–578 (2013).
130. Crochet, S. & Petersen, C. C. H. Correlating whisker behavior with membrane potential in barrel cortex of awake mice. *Nature Neurosci.* **9**, 608–610 (2006).
131. Hafting, T., Fyhn, M., Molden, S., Moser, M.-B. & Moser, E. I. Microstructure of a spatial map in the entorhinal cortex. *Nature* **436**, 801–806 (2005).
132. Burgess, N. Grid cells and theta as oscillatory interference: theory and predictions. *Hippocampus* **18**, 1157–1174 (2008).
133. Burgess, N., Barry, C. & O'Keefe, J. An oscillatory interference model of grid cell firing. *Hippocampus* **17**, 801–812 (2007).
134. Domnisoru, C., Kinkhabwala, A. A. & Tank, D. W. Membrane potential dynamics of grid cells. *Nature* **495**, 199–204 (2013).
135. Schmidt-Hieber, C. & Häusser, M. Cellular mechanisms of spatial navigation in the medial entorhinal cortex. *Nature Neurosci.* **16**, 325–331 (2013).
136. Kim, J. *et al.* mGRASP enables mapping mammalian synaptic connectivity with light microscopy. *Nature Methods* **9**, 96–102 (2012).
137. Spruston, N., Jaffe, D. B. & Johnston, D. Dendritic attenuation of synaptic potentials and currents: the role of passive membrane properties. *Trends Neurosci.* **17**, 161–166 (1994).
138. Epsztein, J., Brecht, M. & Lee, A. K. Intracellular determinants of hippocampal CA1 place and silent cell activity in a novel environment. *Neuron* **70**, 109–120 (2011).
139. Harvey, C. D., Collman, F., Dombeck, D. A. & Tank, D. W. Intracellular dynamics of hippocampal place cells during virtual navigation. *Nature* **461**, 941–946 (2009).
140. Lee, D., Lin, B.-J. & Lee, A. K. Hippocampal place fields emerge upon single-cell manipulation of excitability during behavior. *Science* **337**, 849–853 (2012).
141. Murayama, M. & Larkum, M. E. Enhanced dendritic activity in awake rats. *Proc. Natl Acad. Sci. USA* **106**, 20482–20486 (2009).
142. Murayama, M. *et al.* Dendritic encoding of sensory stimuli controlled by deep cortical interneurons. *Nature* **457**, 1137–1141 (2009).
This paper demonstrates that active sensory stimulation evokes calcium spikes in the dendrites of layer 5 barrel cortex neurons.
143. Xu, N. *et al.* Nonlinear dendritic integration of sensory and motor input during an active sensing task. *Nature* **492**, 247–251 (2012).
144. Osten, P. & Margrie, T. W. Mapping brain circuitry with a light microscope. *Nature Methods* **10**, 515–523 (2013).
145. Denk, W. & Horstmann, H. Serial block-face scanning electron microscopy to reconstruct three-dimensional tissue nanostructure. *PLoS Biol.* **2**, e329 (2004).
146. Helmstaedter, M., Briggman, K. L. & Denk, W. High-accuracy neurite reconstruction for high-throughput neuroanatomy. *Nature Neurosci.* **14**, 1081–1088 (2011).
147. Duemani Reddy, G., Kelleher, K., Fink, R. & Saggau, P. Three-dimensional random access multiphoton microscopy for functional imaging of neuronal activity. *Nature Neurosci.* **11**, 713–720 (2008).
148. Fernández-Alfonso, T. *et al.* Monitoring synaptic and neuronal activity in 3D with synthetic and genetic indicators using a compact acousto-optic lens two-photon microscope. *J. Neurosci. Methods* **222C**, 69–81 (2013).
149. Katona, G. *et al.* Fast two-photon *in vivo* imaging with three-dimensional random-access scanning in large tissue volumes. *Nature Methods* **9**, 201–208 (2012).
150. Poo, C. & Isaacson, J. S. A major role for intracortical circuits in the strength and tuning of odor-evoked excitation in olfactory cortex. *Neuron* **72**, 41–48 (2011).
151. Olcese, U., Iurilli, G. & Medini, P. Cellular and synaptic architecture of multisensory integration in the mouse neocortex. *Neuron* **79**, 579–593 (2013).
152. Hodgkin, A. L. & Rushton, W. A. H. The electrical constants of a crustacean nerve fibre. *Proc. R. Soc. Med.* **134**, 444–479 (1946).
153. Segev, I., Rinzel, J. & Shepherd, G. *The Theoretical Foundation of Dendritic Function: Selected Papers of Wilfrid Rall* (MIT Press, 1995).
154. Spruston, N., Jaffe, D. B., Williams, S. H. & Johnston, D. Voltage- and space-clamp errors associated with the measurement of electrotonically remote synaptic events. *J. Neurophysiol.* **70**, 781–802 (1993).
155. Roth, A. & Häusser, M. Compartmental models of rat cerebellar Purkinje cells based on simultaneous somatic and dendritic patch-clamp recordings. *J. Physiol. (Lond.)* **535**, 445–472 (2001).
156. Williams, S. R. & Mitchell, S. J. Direct measurement of somatic voltage clamp errors in central neurons. *Nature Neurosci.* **11**, 790–798 (2008).
157. Spruston, N. & Johnston, D. Out of control in the dendrites. *Nature Neurosci.* **11**, 733–734 (2008).
158. Sharp, A. A., O'Neil, M. B., Abbott, L. F. & Marder, E. The dynamic clamp: artificial conductances in biological neurons. *Trends Neurosci.* **16**, 389–394 (1993).
159. Robinson, H. P. & Kawai, N. Injection of digitally synthesized synaptic conductance transients to measure the integrative properties of neurons. *J. Neurosci. Methods* **49**, 157–165 (1993).
160. Poleg-Polsky, A. & Diamond, J. S. Imperfect space clamp permits electrotonic interactions between inhibitory and excitatory synaptic conductances, distorting voltage clamp recordings. *PLoS ONE* **6**, e19463 (2011).

Acknowledgements
The authors thank S. Chen for feedback on an earlier version of the manuscript. P.C. is supported a UK Medical Research Council (MRC) Career Development Award (G1000512) and a Human Frontier Science Program Young Investigator Award. A.T.S. is supported by the UK MRC (MC_UP_1202/5). S.R.W. is supported by the Australian Research Council (FT100100502) and the NHMRC (APP1004575). T.W.M. is a Wellcome Trust Investigator and is supported by the UK MRC (MC_U1175975156).

Competing interests statement
The authors declare no competing interests.